JOURNAL OF COMPUTATIONAL PHYSICS 1, 29-50 (1966)

A Computation for Studying the Formation of the Relativistic Electron Layer in Astron[1]

JOHN KILLEEN AND SHIRLEY L. ROMPEL

University of California, Lawrence Radiation Laboratory, Livermore, California

ABSTRACT

In the controlled fusion experiment, Astron, relativistic electrons are injected at the end of a long cylindrical tank across an applied axial magnetic field. A rotating cylindrical sheath of electrons is formed. The self-consistent field problem is solved by integrating the time-dependent Vlasov-Maxwell equations numerically using finite-difference methods. The problem described is four dimensional and requires a large scale computing system for the solution of the difference equations.

INTRODUCTION

In the controlled fusion experiment, Astron [1], relativistic electrons are injected into a cylindrical region containing an applied magnetic field. The object is to form the E-Layer, a cylindrical layer of electrons, so that the self-field exceeds the applied field. It is intended that the resulting configuration will be axially symmetric with no azimuthal component of magnetic field.

The mathematical model for the build-up of the electron layer and self-field is the time-dependent Vlasov equation coupled with Maxwell's equations. Assuming axial symmetry the field component B_r and B_z can be derived from a stream function $\psi(r, z, t)$. The canonical angular momentum, p_θ, is a constant of the motion, and we assume that all

[1] Contract No. W-7405-eng-48.

electrons are injected with the same value of p_θ. Hence we can consider an electron distribution function, f, defined on a four dimensional phase space (r, z, p_r, p_z). We assume that the system is electrically neutral at every point. The ion distribution is not solved explicitly, but ions are assumed to be present providing charge neutralization of the layer.

The partial differential equations for $\psi(r, z, t)$ and $f(r, z, p_r, p_z, t)$ are solved numerically using finite-difference methods. The methods used are described in detail. At each time step an integration of f over velocity space yields the current density $j_\theta(r, z, t)$. The self-field is then computed from the solution of the ψ equation, and added to the applied field, giving the total field used in the Vlasov equation. We are thus solving the self-consistent field problem. The phase space can consist of over 160 000 points, e.g., 81 in z, 12 in r, 19 in p_z, and 9 in p_r. Such a computation has only become feasible since the advent of larger computing machines. The problems described in this paper have been done on the LARC.

A program of this type is meant to be used for extensive parameter studies. In particular, the form of the applied fields can be varied, as well as the method of injection. There is a great variety of quantities that can be printed out or plotted at any given time step. Usually we concentrate on dependent variables which are functions of the spatial coordinates r and z, such as the current density. This together with the magnetic field describes the solution to the self-consistent field problem. Velocity distributions of the electrons can also be plotted. In this report we shall give a sample of displayed output of some results for a convenient form of the vacuum field and a simple mode of injection.

I. Mathematical Model for the Formation of the E-Layer [2]

Although transient radial and axial currents will exist in this model, particularly in the early stages of formation and near the injection point, these are assumed to be small compared with the azimuthal current. The radial and axial components of the magnetic vector potential are therefore neglected. The addition of these components to the present model would not be an unreasonable complication, and has been considered for future computations.

We specify the magnetic field by the single component of the vector potential, $A_\theta(r, z, t)$. The equation for A_θ is

$$\frac{1}{c^2}\frac{\partial^2 A_\theta}{\partial t^2} - \frac{\partial^2 A_\theta}{\partial z^2} - \frac{\partial}{\partial r}\left[\frac{1}{r}\frac{\partial}{\partial r}(rA_\theta)\right] = 4\pi j_\theta, \tag{1}$$

and we have

$$B_r = -\frac{\partial A_\theta}{\partial z}; \quad B_z = \frac{1}{r}\frac{\partial}{\partial r}(rA_\theta); \quad E_\theta = -\frac{1}{c}\frac{\partial A_\theta}{\partial t}. \tag{2}$$

We can write the canonical angular momentum as

$$p_\theta = m_0\gamma r v_\theta + \frac{e}{c} rA_\theta,$$

where $\gamma = (1 - v^2/c^2)^{-1/2}$, m_0 is the electron rest mass, and v_θ is the azimuthal component of velocity.

From the above we have the equation

$$\frac{\gamma}{c} rv_\theta + \frac{e}{m_0c^2} rA_\theta = \frac{p_\theta}{m_0c} = \text{constant}.$$

It is convenient to introduce the function

$$\psi = \frac{\gamma}{c} rv_\theta, \tag{3}$$

so that

$$\psi = \frac{p_\theta}{m_0c} - \frac{e}{m_0c^2} rA_\theta, \tag{4}$$

and since we are assuming that all the electrons have the same p_θ we can use ψ in place of A_θ to determine the field. From Eqs. (1), (2), and (4) we have

$$\frac{1}{c^2}\frac{\partial^2\psi}{\partial t^2} - \frac{\partial^2\psi}{\partial z^2} - r\frac{\partial}{\partial r}\left[\frac{1}{r}\frac{\partial\psi}{\partial r}\right] = -\frac{4\pi e}{m_0c^2} rj_\theta, \tag{5}$$

$$B_r = \frac{m_0c^2}{e}\frac{1}{r}\frac{\partial\psi}{\partial z}; \qquad B_z = -\frac{m_0c^2}{e}\frac{1}{r}\frac{\partial\psi}{\partial r}. \tag{6}$$

We introduce the dimensionless velocity $\mathbf{u}$ defined by

$$\mathbf{u} = \frac{\gamma}{c}\mathbf{v}. \tag{7}$$

The expression for γ becomes

$$\gamma = (1 + u_r^2 + u_\theta^2 + u_z^2)^{1/2},$$

and from (3) we have $\psi = ru_\theta$; hence

$$\gamma = \left(1 + u_r^2 + u_z^2 + \frac{\psi^2}{r^2}\right)^{1/2}. \tag{8}$$

Let $f(r, z, u_r, u_z, t)$ be the electron distribution function in phase space, such that $f(r, z, u_r, u_z, t)\, drdzdu_rdu_z$ is the number of electrons in the element $drdzdu_rdu_z$ at the point (r, z, u_r, u_z) at time t. The dimensions of f are the number of electrons per square centimeter. The equation governing f is

$$\frac{df}{dt} = S(r, z, u_r, u_z, t),$$

where S expresses the source of electrons injected into the phase space. We write the above as

$$\frac{\partial f}{\partial t} + \frac{\partial f}{\partial r}\frac{dr}{dt} + \frac{\partial f}{\partial z}\frac{dz}{dt} + \frac{\partial f}{\partial u_r}\frac{du_r}{dt} + \frac{\partial f}{\partial u_z}\frac{du_z}{dt} = S.$$

From (7) we have

$$\frac{dr}{dt} = \frac{c}{\gamma}u_r \quad \text{and} \quad \frac{dz}{dt} = \frac{c}{\gamma}u_z. \tag{9}$$

We determine du_r/dt and du_z/dt from the relativistic equations of motion of the electrons. The radial and axial equations are

$$m_0(\gamma\ddot{r} + \dot{\gamma}\dot{r} - \gamma r\dot{\theta}^2) = \frac{e}{c} r\dot{\theta} B_z,$$

$$m_0(\gamma\ddot{z} + \dot{\gamma}\dot{z}) = -\frac{e}{c} r\dot{\theta} B_r.$$

From (9) we have

$$\ddot{r} = \frac{c}{\gamma}\dot{u}_r - \frac{c}{\gamma^2}\dot{\gamma} u_r$$

$$\ddot{z} = \frac{c}{\gamma}\dot{u}_z - \frac{c}{\gamma^2}\dot{\gamma} u_z,$$

and using (3) and (6) we have

$$\frac{du_r}{dt} = -\frac{c}{\gamma}\frac{\partial}{\partial r}\left(\frac{\psi^2}{2r^2}\right)$$
$$\frac{du_z}{dt} = -\frac{c}{\gamma}\frac{\partial}{\partial z}\left(\frac{\psi^2}{2r^2}\right). \tag{10}$$

The equation for f can now be written as

$$\frac{\gamma}{c}\frac{\partial f}{\partial t} + u_r\frac{\partial f}{\partial r} + u_z\frac{\partial f}{\partial z} - \frac{\partial}{\partial r}\left(\frac{\psi^2}{2r^2}\right)\frac{\partial f}{\partial u_r} - \frac{\partial}{\partial z}\left(\frac{\psi^2}{2r^2}\right)\frac{\partial f}{\partial u_z} = S\frac{\gamma}{c} \tag{11}$$

The azimuthal current density j_θ is given by

$$j_\theta = \frac{e}{c}\frac{1}{2\pi r}\iint v_\theta f\, du_r\, du_z$$

From (3) we have

$$j_\theta = \frac{e}{2\pi}\frac{\psi}{r^2}\iint \frac{f}{\gamma}\, du_r\, du_z. \tag{12}$$

Equation (5) becomes

$$\frac{1}{c^2}\frac{\partial^2\psi}{\partial t^2} - \frac{\partial^2\psi}{\partial z^2} - r\frac{\partial}{\partial r}\left[\frac{1}{r}\frac{\partial\psi}{\partial r}\right] = -r_e\frac{2\psi}{r}\iint\frac{f}{\gamma}\, du_r\, du_z, \tag{13}$$

where $r_e = e^2/m_0c^2$ is the classical electron radius. Equations (8), (11), and (13) are the self-consistent set of equations that describe the formation of the E-layer.

II. Dimensionless Equations, Boundary Conditions

It is useful in a numerical computation of this type to introduce an appropriate set of dimensionless variables. In place of ψ, given by Eq. (4), we use the variable $\bar{\mu}$ defined by

$$\bar{\mu} = \psi/(p_\theta/m_0c).$$

In order to evaluate the above denominator we consider an equilibrium orbit in the vacuum field. At the midplane, $z = 0$, the end mirror fields are assumed to be negligible, i.e., the vacuum field at $z = 0$ is given by

$$A_\theta(r, 0) = \tfrac{1}{2}B_0r,$$

where B_0 is a constant determined by the injection energy and radius and the desired pitch angle. For an equilibrium orbit at $z = 0$ we have from the radial equation of motion

$$m_0\gamma r_0\dot{\theta}^2 = -\frac{e}{c} r_0\dot{\theta}B_0,$$

where r_0 is the radius of the equilibrium orbit at $z = 0$. Hence

$$p_\theta = -\frac{e}{c} B_0 r_0^2 + \frac{1}{2}\frac{e}{c} B_0 r_0^2 = -\frac{1}{2}\frac{e}{c} B_0 r_0^2,$$

and we have

$$\bar{\mu} = -\frac{2m_0c^2}{eB_0r_0^2}\psi. \tag{14}$$

We introduce the following dimensionless variables

$$R = \frac{r}{r_0} \qquad Z = \frac{z}{r_0} \qquad \tau = \frac{ct}{r_0}$$

$$\bar{a}_\theta = \frac{A_\theta}{B_0 r_0} \qquad \bar{b}_r = \frac{B_r}{B_0} \qquad \bar{b}_z = \frac{B_z}{B_0}$$

From these definitions and Eqs. (4), (6), and (14), we have

$$\bar{\mu} = 1 + 2R\bar{a}_\theta \qquad \bar{b}_r = -\frac{1}{2R}\frac{\partial\bar{\mu}}{\partial Z} \qquad \bar{b}_z = \frac{1}{2R}\frac{\partial\bar{\mu}}{\partial R}$$

It is convenient to let

$$\bar{\mu} = \mu_c + \mu,$$

where μ_c represents the vacuum field and is created by external coils, and μ is the contribution due to the electron layer. The function μ_c satisfies the equation

$$\frac{\partial^2\mu_c}{\partial\tau^2} - \frac{\partial^2\mu_c}{\partial Z^2} - R\frac{\partial}{\partial R}\left(\frac{1}{R}\frac{\partial\mu_c}{\partial R}\right) = 0.$$

We denote the components of the vacuum magnetic field by b_{rc} and b_{zc} and the azimuthal component of the corresponding magnetic potential by $a_{\theta c}$. For the electron distribution functions we use the dimensionless quantity, ϱ, defined by

$$\varrho = r_e r_0 f. \tag{15}$$

We introduce the parameter C_1 given by

$$C_1 = -\frac{eB_0 r_0}{2m_0 c^2} = -(2.93 \times 10^{-4}) B_0 r_0.$$

We define the function $P(R, Z, \tau)$ given by

$$P = \frac{1}{2} C_1^2 \frac{\bar{\mu}^2}{R^2}. \tag{16}$$

This is the potential function for the electron motion, and the equations of motion in these variables become

$$\gamma \frac{du_r}{d\tau} = -\frac{\partial P}{\partial R} \qquad \gamma \frac{du_z}{d\tau} = -\frac{\partial P}{\partial Z}.$$

We can now give the complete set of equations in dimensionless form. Equation (13) becomes

$$\frac{\partial^2 \mu}{\partial \tau^2} - \frac{\partial^2 \mu}{\partial Z^2} - R \frac{\partial}{\partial R}\left(\frac{1}{R}\frac{\partial \mu}{\partial R}\right) = -\frac{2\bar{\mu}}{R} \iint \frac{\varrho}{\gamma} du_r\, du_z. \tag{17}$$

Equation (11) becomes

$$\frac{\partial \varrho}{\partial \tau} + \frac{u_r}{\gamma}\frac{\partial \varrho}{\partial R} + \frac{u_z}{\gamma}\frac{\partial \varrho}{\partial Z} - \frac{P_r}{\gamma}\frac{\partial \varrho}{\partial u_r} - \frac{P_z}{\gamma}\frac{\partial \varrho}{\partial u_z} = \sigma, \tag{18}$$

where

$$\sigma = r_e r_0^2 \frac{S}{c} = (2.82 \times 10^{-13}) r_0^2 \frac{S}{c} \tag{19}$$

$$P_r = \frac{\partial P}{\partial R} = C_1^2 \left[\frac{2}{R}\bar{\mu}\bar{b}_z - \frac{1}{R^3}\bar{\mu}^2\right] \tag{20}$$

$$P_z = \frac{\partial P}{\partial Z} = C_1^2 \left[-\frac{2}{R}\bar{\mu}\bar{b}_r\right] \tag{21}$$

$$\bar{b}_r = b_{rc} - \frac{1}{2R}\frac{\partial \mu}{\partial Z} \tag{22}$$

$$\bar{b}_z = b_{zc} + \frac{1}{2R}\frac{\partial \mu}{\partial R} \tag{23}$$

$$\gamma = (1 + u_r^2 + u_z^2 + 2P)^{1/2}. \tag{24}$$

We wish to solve the initial value problem given by (17) and (18) together with Eqs. (19)–(24). At time $t = 0$, we have

$$\bar{\mu} = \mu_c = 1 + 2Ra_{\theta c}.$$

Hence, the initial condition for Eq. (17) is

$$\mu(R, Z, 0) = 0.$$

We solve the equation on the domain

$$0 \leq R \leq R_{\max}, \qquad -l^* \leq Z \leq l^*,$$

where $l^* = l/r_0$ and $R_{\max}$ is chosen sufficiently large so that the effect of the electron layer can be neglected. The boundary conditions are those of conducting walls, given by

$$\mu(R_{\max}, Z, \tau) = 0, \qquad \mu(R, -l^*, \tau) = 0, \qquad \mu(R, l^*, \tau) = 0.$$

In many problems we assume that the solution is symmetric about $Z = 0$ and solve in the domain $0 \leq Z \leq l^*$. The boundary condition at $Z = 0$ is then

$$\frac{\partial \mu}{\partial Z} = 0$$

The initial condition for Eq. (18) is

$$\varrho(R, Z, u_r, u_z, 0) = 0.$$

We solve the equation on the domain

$$R_1 \leq R \leq R_2, \qquad -l^* \leq Z \leq l^*$$
$$-(u_r)_{\max} \leq u_r \leq (u_r)_{\max}, \qquad -(u_z)_{\max} \leq u_z \leq (u_z)_{\max}$$

where R_1 and R_2 are the radii of the inner and outer material walls, respectively, of the cylindrical region where the electron layer is formed. The velocity space, i.e., $(u_r)_{\max}$ and $(u_z)_{\max}$, is taken large enough to accommodate all but the high velocity tail of the electron distribution function. This is small because electrons of too high a velocity would leave the system. The boundary condition on ϱ is that $\varrho = 0$ on all the boundaries of the four-dimensional domain. In the case of the domain $0 \leq Z \leq l^*$ we assume that the electron distribution function is sym-

metric about the plane $Z = 0$, i.e., as many electrons are going in one direction as the reverse. For this to apply at all times implies equal injection at both ends.

III. Finite-Difference Methods

In this section we give the finite-difference approximations used in the LARC code LAYER. We subdivide the phase space into the finite-difference mesh given by $Z_i = ih$, $R_j = jh$, $(u_z)_k = kh^*$, $(u_r)_l = lh^*$, where i, j, k, and l are integers. We have $-I \leq i \leq I$, $0 \leq j \leq J$, $-K \leq k \leq K$, $-L \leq l \leq L$, where $Ih = l^*$, $Jh = R_{\max}$, $Kh^* = (u_z)_{\max}$, $Lh^* = (u_r)_{\max}$. Let $\tau_n = n\Delta\tau$, with $n = 0, 1, 2, 3, \ldots$ and introduce, the notation $\mu^n_{i,j} = \mu(R_j, Z_i, \tau_n)$, and $\varrho^n_{i,j,k,l} = \varrho(R_j, Z_i, u_{rl}, u_{zk}, \tau_n)$.

We solve Eq. (17) by an alternating direction implicit method. For stability reasons we found it convenient to use half-time steps for this equation. The difference approximation is then written as two equations. In the first half-time step the equation is implicit in the R direction and explicit in the Z direction; in the second half-time step it is implicit in the Z direction and explicit in the R direction. The difference equations are

$$\frac{\mu^{n+1/2}_{i,j} - 2\mu^n_{i,j} + \mu^{n-1/2}_{i,j}}{(\Delta t/2)^2} = \frac{2j}{h^2}\left[\frac{\mu^{n+1/2}_{i,j+1} - \mu^{n+1/2}_{i,j}}{2j+1} - \frac{\mu^{n+1/2}_{i,j} - \mu^{n+1/2}_{i,j-1}}{2j-1}\right] + \frac{\mu^n_{i+1,j} - 2\mu^n_{i,j} + \mu^n_{i-1,j}}{h^2} + \bar{I}^n_{i,j}, \tag{25}$$

and

$$\frac{\mu^{n+1}_{i,j} - 2\mu^{n+1/2}_{i,j} + \mu^n_{i,j}}{(\Delta t/2)^2} = \frac{\mu^{n+1}_{i+1,j} - 2\mu^{n+1}_{i,j} + \mu^{n+1}_{i-1,j}}{h^2} + \bar{I}^{n+1/2}_{i,j} + \frac{2j}{h^2}\left[\frac{\mu^{n+1/2}_{i,j+1} - \mu^{n+1/2}_{i,j}}{2j+1} - \frac{\mu^{n+1/2}_{i,j} - \mu^{n+1/2}_{i,j-1}}{2j-1}\right]. \tag{26}$$

We have $\bar{\mu}^n_{i,j} = (\mu_c)_{i,j} + \mu^n_{i,j}$, where μ_c represents the applied field, and

$$\bar{I}^n_{i,j} = -2\frac{\bar{\mu}^n_{i,j}}{jh}(h^*)^2 \sum_{k=-K}^{K} \sum_{l=-L}^{L} \frac{\varrho^n_{i,j,k,l}}{\gamma^n_{i,j,k,l}} \tag{27}$$

$$\gamma^n_{i,j,k,l} = [1 + (kh^*)^2 + (lh^*)^2 + C_1^2(jh)^{-2}(\bar{\mu}^n_{i,j})^2]^{1/2}. \tag{28}$$

The expression for $\bar{I}^{n+1/2}_{i,j}$ uses the same sum over k and l but replaces $\bar{\mu}^n_{i,j}$ by $\bar{\mu}^{n+1/2}_{i,j}$.

We can write the above difference approximation as two sets of linear algebraic equations:

$$\begin{aligned} -a_j\mu^{n+1/2}_{i,j+1} + (a_j + b_j + \Lambda)\mu^{n+1/2}_{i,j} - b_j\mu^{n+1/2}_{i,j-1} \\ = \mu^n_{i+1,j} - (2 - 2\Lambda)\mu^n_{i,j} + \mu^n_{i-1,j} + h^2\bar{I}^n_{i,j} - \Lambda\mu^{n-1/2}_{i,j}, \end{aligned} \tag{29}$$

and

$$\begin{aligned} -\mu^{n+1}_{i+1,j} + (2 + \Lambda)\mu^{n+1}_{i,j} - \mu^{n+1}_{i-1,j} = a_j\mu^{n+1/2}_{i,j+1} - (a_j + b_j - 2\Lambda)\mu^{n+1/2}_{i,j} \\ + b_j\mu^{n+1/2}_{i,j-1} + h^2\bar{I}^{n+1/2}_{i,j} - \Lambda\mu^n_{i,j}, \end{aligned} \tag{30}$$

where

$$\Lambda = \left(\frac{2h}{\Delta t}\right)^2; \qquad a_j = \frac{2j}{2j+1}; \qquad b_j = \frac{2j}{2j-1}.$$

The method for solving the systems is a standard one [3, 4]. For the first half-time step we use the algorithm

$$\mu^{n+1/2}_{i,j} = E^{1/2}_{i,j}\,\mu^{n+1/2}_{i,j+1} + f^n_{i,j} \tag{31}$$

for all i and $j = 0, 1, 2, 3, \ldots, J-1$,
where

$$E^{1/2}_{i,j} = \frac{a_j}{a_j + b_j + \Lambda - b_jE^{1/2}_{i,j-1}}$$

$$f^n_{i,j} = \frac{\delta^n_{i,j} + b_jf^n_{i,j-1}}{a_j + b_j + \Lambda - b_jE^{1/2}_{i,j-1}}$$

$$\delta^n_{i,j} = \mu^n_{i+1,j} - (2 - 2\Lambda)\mu^n_{i,j} + \mu^n_{i-1,j} + h^2\bar{I}^n_{i,j} - \Lambda\mu^{n-1/2}_{i,j}$$

for all i and $j = 1, 2, 3, \ldots, J-1$. We use the boundary condition at $R = 0$ to give

$$E^{1/2}_{i,0} = 0 \quad \text{and} \quad f^n_{i,0} = 0$$

for all i. The computation consists of a double sweep along each i line; on the first sweep the E's and f's are calculated, and on the second sweep the μ's are calculated using Eq. (31) and the boundary value

$$\mu^{n+1/2}_{i,J} = 0 \quad \text{for all } i.$$

For the second half-time step we use the algorithm

$$\mu_{i,j}^{n+1} = E_{i,j}^{1}\mu_{i+1,j}^{n+1} + f_{i,j}^{n+1/2} \tag{32}$$

for all j and $-I \leq i \leq I-1$ (or $0 \leq i \leq I-1$), where

$$E_{i,j}^{1} = \frac{1}{2 + \Lambda - E_{i-1,j}^{1}}$$

$$f_{i,j}^{n+1/2} = \frac{\delta_{i,j}^{n+1/2} + f_{i-1,j}^{n+1/2}}{2 + \Lambda - E_{j-1,j}^{1}}$$

$$\delta_{i,j}^{n+1/2} = a_j\mu_{i,j+1}^{n+1/2} - (a_j + b_j - 2\Lambda)\mu_{i,j}^{n+1/2} + b_j\mu_{i,j-1}^{n+1/2} + h^2\bar{I}_{i,j}^{n+1/2} - \Lambda\mu_{i,j}^{n}$$

for all j and $-I+1 \leq i \leq I-1$ (or $1 \leq i \leq I-1$). We use the boundary condition at $Z = -l^*$ to give

$$E_{-I,j}^{1} = 0 \quad \text{and} \quad f_{-I,j}^{n+1/2} = 0$$

for all j. For a single ended problem the condition at $Z = 0$ yields $E_{0,j}^{1} = 1, f_{0,j}^{n+1/2} = 0$ for all j. The computational procedure is again a double sweep using Eq. (32) and the boundary value

$$\mu_{I,j}^{n+1} = 0 \quad \text{for all } j.$$

This implicit scheme may seem elaborate compared with an explicit scheme; however, the simpler method was tried originally and did not give as good results. Furthermore, the time required for solution of the μ-equation is very small compared with the time required for the solution of the four dimensional ϱ-equation as we shall see. By using the implicit difference method for Eq. (17) we have been able to double Δt, which for a calculation of this type saves many hours of machine time.

At the end of a full-time step the magnetic field is calculated at each point in the (r, z) domain. From Eqs. (22) and (23) we have

$$(\bar{b}_r)_{i,j}^{n} = (b_{rc})_{i,j} - (4jh^2)^{-1}[\mu_{i+1,j}^{n} - \mu_{i-1,j}^{n}] \tag{33}$$

$$(\bar{b}_z)_{i,j}^{n} = (b_{zc})_{i,j} + (4jh^2)^{-1}[\mu_{i,j+1}^{n} - \mu_{i,j-1}^{n}]. \tag{34}$$

The vacuum field expressions b_{rc} and b_{zc} are given and will be discussed later. The above field components, $\bar{b}_r$ and $\bar{b}_z$, are printed and plotted output respectively; in addition they are used to compute P_r and P_z,

which are needed in the solution of Eq. (18). From Eqs. (20) and (21) we have

$$(P_r)^n_{i,j} = C_1^2[2(jh)^{-1}\bar{\mu}^n_{i,j}(\bar{b}_z)^n_{i,j} - (jh)^{-3}(\bar{\mu}^n_{i,j})^2] \tag{35}$$

$$(P_z)^n_{i,j} = -C_1^2[2(jh)^{-1}\bar{\mu}^n_{i,j}(\bar{b}_r)^n_{i,j}], \tag{36}$$

where $\bar{\mu}^n_{i,j} = (\mu_c)_{i,j} + \mu^n_{i,j}$.

We shall now consider the solution of Eq. (18) by finite difference methods. To illustrate the problem consider the one-dimendional equation

$$\frac{\partial \varrho}{\partial \tau} + u\frac{\partial \varrho}{\partial x} = 0, \qquad u = \text{constant}. \tag{37}$$

The simplest two-level approximation would be

$$\varrho^{n+1}_j = \varrho^n_j - \tfrac{1}{2}\alpha(\varrho^n_{j+1} - \varrho^n_{j-1}),$$

where $\alpha = u\Delta\tau/\Delta x$. This scheme is unstable no matter how small $\Delta\tau$ is. The simplest alternative is

$$\begin{aligned}\varrho^{n+1}_j &= \varrho^n_j - \alpha(\varrho^n_j - \varrho^n_{j-1}), \qquad u \geq 0\\ &= \varrho^n_j - \alpha(\varrho^n_{j+1} - \varrho^n_j), \qquad u < 0.\end{aligned}$$

This scheme is stable so long as $|\alpha| \leq 1$. The generalization of this to Eq. (18) is straightforward and leads to the stability conditions

$$\frac{kh^*\Delta\tau}{\gamma h} \leq 1, \quad \frac{lh^*\Delta\tau}{\gamma h} \leq 1, \quad \frac{P_z\Delta\tau}{\gamma h^*} \leq 1, \quad \frac{P_r\Delta\tau}{\gamma h^*} \leq 1. \tag{38}$$

The first version of the LAYER code employed this scheme and an explicit approximation to Eq. (17). Unfortunately the above scheme introduces an artificial diffusion which spoils the results after a short time.

We can consider a space an time centered three-level approximation to Eq. (37):

$$\varrho^{n+1}_j = \varrho^{n-1}_j - \alpha(\varrho^n_{j+1} - \varrho^n_{j-1})$$

which is stable if $|\alpha| \leq 1$. The extension to more than one dimension is again immediate, leading to the stability condition Eq. (38). The second version of LAYER used this scheme. Considerable computation has been done with this method leading to fairly satisfactory results, but with the crude mesh employed in this problem it is still not accurate enough for extremely long running times. Furthermore, it has the dis-

advantage of being a three-level formula, and when the time step must be decreased for stability reasons it is quite awkward.

The third version of LAYER uses a three-point approximation to the advective term. For Eq. (37) this becomes

$$\varrho_j^{n+1} = \varrho_j^n - \tfrac{1}{2}\alpha(\varrho_{j+1}^n - \varrho_{j-1}^n) + \tfrac{1}{2}\alpha^2(\varrho_{j+1}^n - 2\varrho_j^n + \varrho_{j-1}^n).$$

This scheme is stable if $|\alpha| \leq 1$. It is accurate to second order in the quantities $u\Delta\tau$ and Δx, and has the convenience of being a two-level formula. The extension to more than one dimension is not straightforward and can lead to an unstable method if not done correctly [5]. We can write the above approximation in matrix form as $\varrho^{n+1} = (I + A)\varrho^n$. If we consider a two-dimensional equation and take the approximation given by the equation $\varrho^{n+1} = (I + A + B)\varrho^n$, where B is the advective difference operator in the other direction, the scheme is unstable. However, if we use the operator equation $\varrho^{n+1} = (I + A)(I + B)\varrho^n$ the scheme is stable. This is the scheme that is used in the third version of LAYER. The difference equation can be represented by

$$\varrho^{n+1} = (I + A)(I + B)(I + C)(I + D)\varrho^n.$$

The computational process involved in a single time step is divided into four cycles. In the first cycle advection in the Z direction is calculated, then in the R direction using the results of the first cycle, then in the u_z direction using the results of the second cycle, and, finally, in the u_r direction using the results of the third cycle. The actual difference equations for Eq. (18) are given below; the fractional time notation is used as a convenient labeling of the cycles and does not represent fractional time steps.

$$\varrho_{i,j,k,l}^{n+1/4} = \varrho_{i,j,k,l}^n - \frac{1}{2}\left(\frac{kh^*\Delta\tau}{h\gamma_{i,j,k,l}^n}\right)(\varrho_{i+1,j,k,l}^n - \varrho_{i-1,j,k,l}^n) + \frac{1}{2}\left(\frac{kh^*\Delta\tau}{h\gamma_{i,j,k,l}^n}\right)^2(\varrho_{i+1,j,k,l}^n - 2\varrho_{i,j,k,l}^n + \varrho_{i-1,j,k,l}^n) \tag{39a}$$

$$\varrho_{i,j,k,l}^{n+1/2} = \varrho_{i,j,k,l}^{n+1/4} - \frac{1}{2}\left(\frac{lh^*\Delta\tau}{h\gamma_{i,j,k,l}^n}\right)(\varrho_{i,j+1,k,l}^{n+1/4} - \varrho_{i,j-1,k,l}^{n+1/4}) + \frac{1}{2}\left(\frac{lh^*\Delta\tau}{h\gamma_{i,j,k,l}^n}\right)^2(\varrho_{i,j+1,k,l}^{n+1/4} - 2\varrho_{i,j,k,l}^{n+1/4} + \varrho_{i,j-1,k,l}^{n+1/4}) \tag{39b}$$

$$\varrho^{n+3/4}_{i,j,k,l} = \varrho^{n+1/2}_{i,j,k,l} - \frac{1}{2}\left(\frac{-(P_z)^n_{i,j}\Delta\tau}{h^*\gamma^n_{i,j,k,l}}\right)(\varrho^{n+1/2}_{i,j,k+1,l} - \varrho^{n+1/2}_{i,j,k-1,l})$$

$$+ \frac{1}{2}\left(\frac{(P_z)^n_{i,j}\Delta\tau}{h^*\gamma^n_{i,j,k,l}}\right)^2(\varrho^{n+1/2}_{i,j,k+1,l} - 2\varrho^{n+1/2}_{i,j,k,l} + \varrho^{n+1/2}_{i,j,k-1,l}) \tag{39c}$$

$$\varrho^{n+1}_{i,j,k,l} = \varrho^{n+3/4}_{i,j,k,l} - \frac{1}{2}\left(\frac{-(P_r)^n_{i,j}\Delta\tau}{h^*\gamma^n_{i,j,k,l}}\right)(\varrho^{n+3/4}_{i,j,k,l+1} - \varrho^{n+3/4}_{i,j,k,l-1})$$

$$+ \frac{1}{2}\left(\frac{(P_r)^n_{i,j}\Delta\tau}{h^*\gamma^n_{i,j,k,l}}\right)^2(\varrho^{n+3/4}_{i,j,k,l+1} - 2\varrho^{n+3/4}_{i,j,k,l} + \varrho^{n+3/4}_{i,j,k,l-1}). \tag{39d}$$

The stability conditions for this finite-difference method are given by Eq. (38).

Since the finite-difference mesh of the four-dimensional phase space consists of such a large number of points, only a small part of it can be in the core storage at any one time; the rest of it is on magnetic drums. The ϱ's of four i strips and the γ's of one i strip are in core storage, i.e., for a fixed value of i: $\gamma^n_{i,j,k,l}$, $\varrho^n_{i,j,k,l}$, $\varrho^n_{i-1,j,k,l}$, $\varrho^n_{i+1,j,k,l}$, for all j, k, l are used to compute $\varrho^{n+1/4}_{i,j,k,l}$ all j, k, l. The $\varrho^{n+1/2}_{i,j,k,l}$, are then computed and stored on top of the $\varrho^n_{i-1,j,k,l}$, which are no longer needed; then the $\varrho^{n+3/4}_{i,j,k,l}$ are computed and stored on top of the $\varrho^{n+1/4}_{i,j,k,l}$, and finally the $\varrho^{n+1}_{i,j,k,l}$ are computed and stored on top of the $\varrho^{n+1/2}_{i,j,k,l}$. Before passing on to the next value of i the contributions to the various integrals such as $\bar{I}$ and the conservation checks are added in. When the ϱ cycles are completed for all values of i the μ equation can be solved, completing the self-consistent solution for that time step.

We must consider the boundary conditions for the ϱ equation and the conservation of particles. Particles can be lost at the physical boundaries $Z = l^*$, $Z = -l^*$, $R = R_1$, and $R = R_2$. Numerically they can also be lost at the boundaries of the velocity domain.

For $i = I$ ($Z = +l^*$) we take $\varrho^{n+1}_{I+1,j,k,l} = 0$, all j, k, l, and compute $\varrho^{n+1}_{I,j,k,l}$ from the above equations. For $k > 0$, $\varrho^{n+1}_{I,j,k,l}$ is added to the sum

$$M^{n+1} = \Delta thh^{*2}\sum_{m=1}^{n+1}\sum_{k=1}^{K}\sum_{l=-L}^{+L}\sum_{j=1}^{J}\varrho^m_{I,j,k,l}, \tag{40}$$

and then set to zero before the next time step. The sum M is the total number of particles lost at $Z = +l^*$. A similar treatment is made

at $i = -I\,(Z = -l^*)$ for $k < 0$. For a single-ended problem with $0 \leq Z \leq l^*$ we use $\varrho^{n+1}_{1-j,k,l} = \varrho^{n+1}_{1,j,-k,l}$ in the computation of $\varrho^{n+1}_{0,j,k,l}$.

At the boundary $R = R_2$ let $R_2 = J_\varrho h$; then we take $\varrho^{n+1}_{i,J_\varrho+1,k,l} = 0$, all i, k, l and $\varrho^{n+1}_{i,J_\varrho,k,l}$ can be computed from the ϱ equations. For $l > 0$, $\varrho^{n+1}_{i,J_\varrho,k,l}$ is added to the sum

$$Q^{n+1} = .1thh^{*2} \sum_{m=1}^{n+1} \sum_{k=-K}^{+K} \sum_{l=0}^{+L} \sum_{i=-I}^{I} \varrho^{m}_{i,J_\varrho,k,l} \tag{41}$$

and then set to zero before the next time step. The sum Q is the total number of particles lost at $R = R_2$. A similar treatment is made at $R = R_1$. In addition to the sums M and Q of particles lost at the material boundaries, a sum of particles injected and a sum of particles in the mesh are computed. Conservation of particles is then checked. Particle energy and field energy are also computed, and conservation of energy is checked. The details of these calculations are given in the Appendix.

IV. Numerical Results

There are two optional forms of the applied magnetic field available in the LAYER code. One form is given by

$$a_{\theta c} = A_1 R + A_2 I_1(\lambda R) \cos \lambda Z \tag{42a}$$

$$b_{rc} = \lambda A_2 I_1(\lambda R) \sin \lambda Z \tag{42b}$$

$$b_{zc} = 2A_1 + \lambda A_2 I_0(\lambda R) \cos \lambda Z, \tag{42c}$$

where I_0 and I_1 are modified Bessel functions of the first kind and λ, A_1, A_2 are given constants.

Another form is

$$a_{\theta c} = \frac{R}{2} + \frac{\alpha}{\lambda} J_1(\lambda R) \exp(-\lambda l^*) \cosh \lambda Z \tag{43a}$$

$$b_{rc} = -\alpha J_1(\lambda R) \exp(-\lambda l^*) \sinh \lambda Z \tag{43b}$$

$$b_{zc} = 1 + \alpha J_0(\lambda R) \exp(-\lambda l^*) \cosh \lambda Z, \tag{43c}$$

where J_0 and J_1 are Bessel functions of the first kind, and λ and α are given constants. An advantage of the above expression is that, if λ satisfies the equation

$$\lambda J_0(\lambda) = J_1(\lambda),$$

then $P_r = 0$ at $R = 1$ for all Z. Hence, if we inject at $R = 1$ with $u_r = 0$ the particles will not spread radially in the early formation of the electron layer. We are injecting at the bottom of a potential trough as shown in Fig. 1. Of course as the self-field develops P_r will no longer be zero at

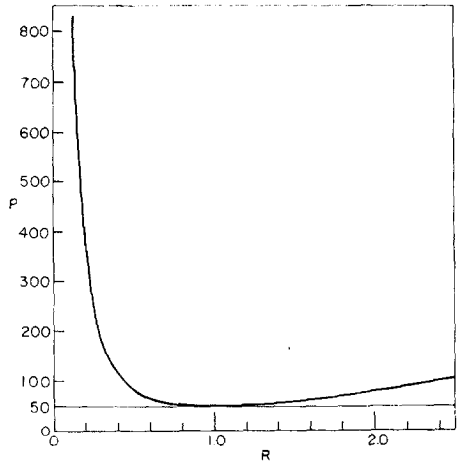

FIG. 1. The magnetic potential, P, as a function of R, at $Z = 0$, for the case $\delta = -60°$.

$R = 1$, and the layer will spread radially. We determine α by the desired pitch angle in the midplane. Consider an equilibrium particle orbit, $R = 1$, with velocity components in the midplane, $Z = 0$, given by

$$(\dot{R},\ R\dot{\theta},\ \dot{Z}) = (0,\ v \sin \delta,\ v \cos \delta);$$

then for such an orbit to be reflected at $Z = l^*$ requires

$$\alpha = -2\lambda(\csc \delta + 1)/J_1(\lambda).$$

We shall present results for the case $\delta = -60°$.

The constant B_0 defined earlier can be given by

$$B_0 = -\frac{m_0 c^2 \gamma \beta}{e r_0} \sin \delta,$$

where β and γ are determined by the injection energy. With B_0 and r_0 we can determine the parameter C_1 used in Eqs. (16), (20), and (21). For $r_0 = 30$ cm and $B_0 = 600$ gauss we have $C_1 = -5.27$. In the calculations shown in this paper we have used $C_1 = -5.0$.

For $r_0 = 30$ cm, we have $l^* = 10.0$, giving a domain $-10 \leq Z \leq 10$. With the vacuum field given by Eq. (43) there is a long central region with uniform axial field. In order to shorten the computation time and still keep a small h we generally halve the above domain. In the problem shown in this report we have used $-5 \leq Z \leq 5$. We have also used $R_2 = 1.5$, $R_1 = 0.5$, $(u_z)_{\max} = 10.0$, $(u_r)_{\max} = 5.0$. The finite-difference mesh is characterized by $h = 1/8$ and $h^* = 1$. The choice of $h = 1/8$ gives a spatial increment of 3.75 cm. The finite-difference phase space is then 81 in Z, 9 in R, 21 in u_z, and 11 in u_r.

The time step, $\Delta\tau$, is governed by the stability conditions given in Eq. (38). The dominant condition is

$$\frac{P_r \Delta\tau}{\gamma h^*} \leq 1.$$

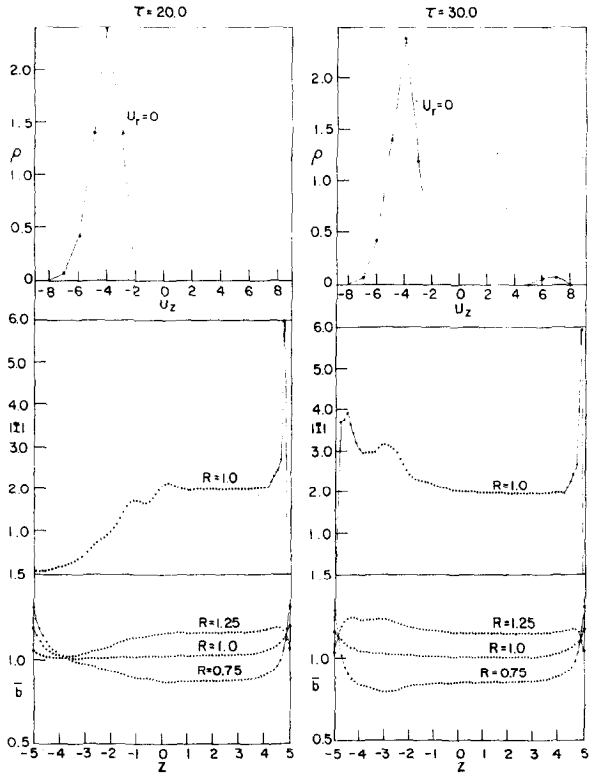

FIG. 2. The current density and the magnitude of the magnetic field as a function of Z for various values of R at $\tau = 20$ and $\tau = 30$. The electron distribution function as a function of u_z for $u_r = 0$ at the point $Z = 0$, $R = 1$, and at $\tau = 20$, $\tau = 30$.

We see from Eq. (20) and Fig. 1 that $|P_r|$ becomes very large for small R. This imposes a practical lower bound on R for reasonable running times. A useful technique is to run for quite a while with some value of R_1, and then as the radial spreading becomes appreciable we can decrease R_1, but must also decrease $\Delta\tau$; e.g., with $h^* = 1$ for $j_{\min} = 5$ we use $\Delta\tau = 0.1$ and for $j_{\min} = 4$ we use $\Delta\tau = 0.05$.

The source of electrons is described by the function σ in Eq. (19). For these calculations we have injected at one point in phase space; e.g., at the point $i = 38$, $j = 8$, $k = 0$, $l = 0$ and amount $\sigma\Delta\tau$ is added at every time step. If 100 A of electrons are injected into a volume of phase space $h^2h^{*2} = (1/8)^2(30)^2$ cm^2, then $S = 0.4466 \times 10^{20}$ elec/cm^2-sec and $S/c = 1.489 \times 10^9$ elec/cm^3. We then have $\sigma = 0.3776$, and for 150 A

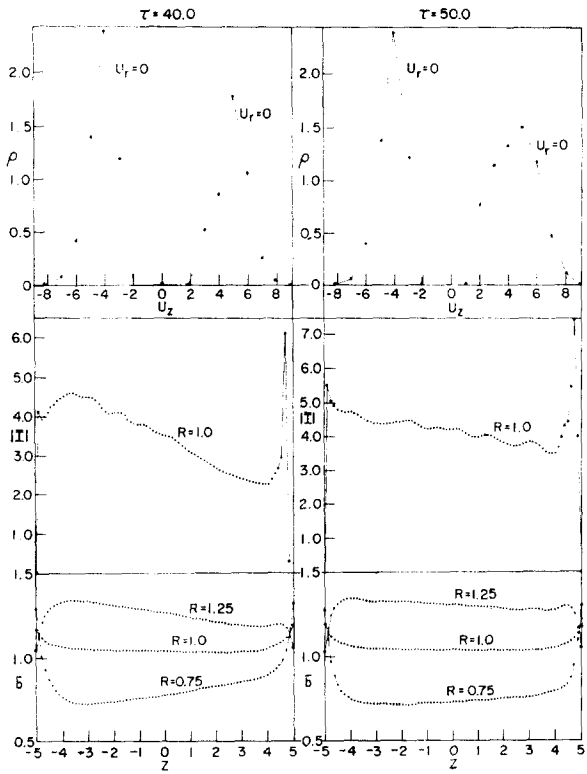

FIG. 3. The current density and the magnitude of the magnetic field as a function of Z for various values of R at $\tau = 40$ and $\tau = 50$. The electron distribution function as a function of u_z for $u_r = 0$ at the point $Z = 0$, $R = 1$, and at $\tau = 40$, $\tau = 50$.

we have $\sigma = 0.5664$. We typiaclly use $\sigma = 0.5$, or to achieve strong self-fields we increase it by an order of magnitude or more.

The case $\delta = -60^{\circ}$ is meant to achieve a pitch angle of 30° in the midplane. In Figs. 2 and 3 we show the early formation of a sharp E-layer, i.e., $P_r = 0$ at $R = 1.0$. The quantity $\bar{I}(R, Z, \tau)$ is given by Eq. (27), and we relate it to the current density by the relation

$$rj_\theta = -(B_0/8\pi)\bar{I}.$$

We also show $\bar{b}(R, Z, \tau)$, where $\bar{b} = (\bar{b}_r^2 + \bar{b}_z^2)^{1/2}$. In these calculations we have used $\sigma = 5.0$ in order to achieve an exaggerated effect on the field in a short time. The electrons are injected at $Z = +4.75$, $R = 1.0$

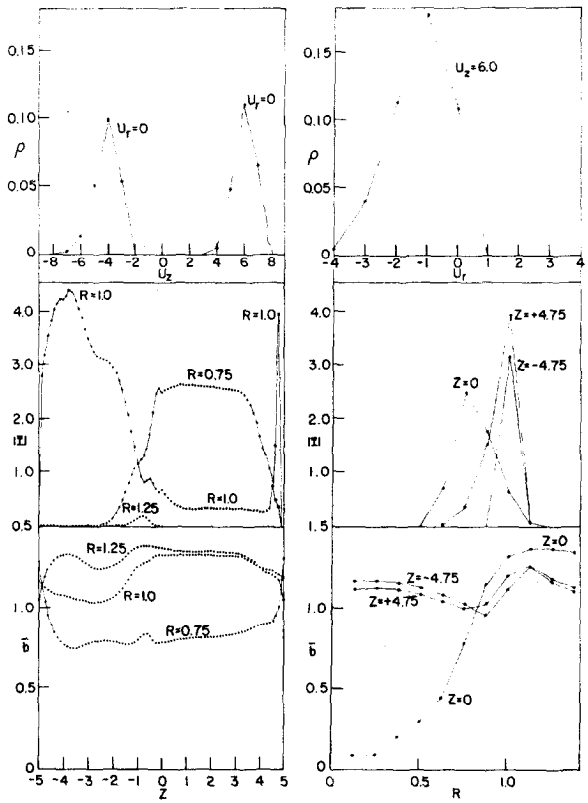

FIG. 4. The current density and the magnitude of the magnetic field as a function of Z for various values of R and as a function of R for various values of Z all at the same time. The electron distribution function as a function of u_z for $u_r = 0$, and as a function of u_r for u_z corresponding to the maximum ϱ, at the point $Z = 0$, $R = 1$.

with $u_r = u_z = 0$. The applied mirror field causes the particles to move to the left. In Fig. 2 we see that at $\tau = 20$ the layer has formed about half way. At this time we also show ϱ vs. u_z at the point $Z = 0$, $R = 1$, and the distribution has a single peak for $u_z < 0$. At $\tau = 30$ the layer has reached the other end and has been reflected by the mirror field. The velocity distribution now shows a small peak for $u_z > 0$. In Fig. 3 we show the same quantities at $\tau = 40$ and $\tau = 50$. The layer has developed for all Z and we see two peaks in the u_z distribution as one would expect.

In Fig. 4 we show the character of the layer after radial spreading has taken place. We see that the layer has moved inward radially in the central region. The reduction of the field in the central region is substantial. The velocity distribution at $Z = 0$, $R = 1$ shows that the maximum is no longer at $u_r = 0$, but has shifted to $u_r < 0$.

Many other runs have been performed with this program for a variety of injection conditions and several versions of the applied magnetic field.

Appendix

Computation Checks

We can give the total number of particles injected into the system at time t by the expression

$$\Delta u_r \Delta u_z \Delta r \Delta z \int_0^t S\, dt',$$

where $\Delta u_r \Delta u_z \Delta r \Delta z$ is the element of phase space used for injection. For the mode of injection described earlier we compute the dimensionless quantity

$$N^n = h^{*2} h^2 \sum_{m=1}^{n} \sigma^m \Delta\tau_m.$$

The total number of particles in the system at time $t = t_n$ is proportional to

$$SUM^n = h^{*2} h^2 \sum_{i=-I}^{I} \sum_{j=1}^{J} \sum_{k=-K}^{K} \sum_{l=-L}^{L} \varrho^n_{i,j,k,l}.$$

We should then have

$$SUM^n + M^n + Q^n = N^n$$

for conservation of particles, where M and Q are the total number of particles lost through the physical boundaries and are defined in Eqs. (40) and (41).

We define the energy in the electromagnetic field by the expression

$$\frac{1}{8\pi}\int_0^{2\pi} d\theta \int_{-l}^{+l} dz \int_0^{r_{\max}} r\, dr[B^2 + E^2].$$

If we divide the above expression by the constant $r_0^3 B_0^2/4$ we obtain the quantity

$$F(t) = \int_{-l^*}^{l^*} dZ \int_0^{R_{\max}} R\, dR[\bar{b}_r^2 + \bar{b}_z^2 + e^2],$$

where $\bar{e}_\theta = E_\theta/B_0 = -(1/2R)(\partial\bar{\mu}/\partial\tau)$.

A finite-difference approximation to this integral is

$$F^n = h^3 \sum_{i=-I}^{I} \sum_{j=0}^{J} j\{[(\bar{b}_r)_{i,j}^n]^2 + [(\bar{b}_z)_{i,j}^n]^2 + [(e_\theta)_{i,j}^n]^2\}.$$

The energy of injected particles can be defined by

$$m_0 c^2 \Delta u_r \Delta u_z \Delta r \Delta z \int_0^t \gamma S\, dt'.$$

If we divide the above by $r_0^3 B_0^2/4$ and use the mode of injection described we have

$$T^n = C_1^{-2} h^{*2} h^2 \sum_{m=1}^{n} \gamma_{inj}^m \sigma^m \Delta\tau_m,$$

where γ_{inj}^m is the γ of the element that the particles are injected into. The energy of particles in the system is given by

$$m_0 c^2 \int\int\int\int \gamma\, f\, dr\, dz\, du_r\, du_z.$$

Again dividing by $r_0^3/B_0^2/4$ we can compute the dimensionless quantity

$$E^n = C_1^{-2} h^{*2} h^2 \sum_{i=-I}^{I} \sum_{j=1}^{J} \sum_{k=-K}^{K} \sum_{l=-L}^{L} \gamma_{i,j,k,l}^n \varrho_{i,j,k,l}^n.$$

The conservation check is then

$$F^n - F^0 + E^n = T^n.$$

These integrals as discussed are really not as accurate as the solutions of the difference equations. Integration formulas which are more sophisticated than the simple sums described must be used to give good conservation checks.

References

1. N. C. Christofilos, *Proc. Intern. Conf. Peaceful Uses At. Energy, Geneva,* 1958, 32, p. 279. Columbia Univ. Press, New York (1958).
2. This mathematical model was first proposed by Dr. Leslie G. Peck in a private communication (1960).
3. D. W. Peacemann and H. H. Rachford, Jr., *J. Soc. Ind. Appl. Math.* **3**, 28 (1955).
4. R. D. Richtmyer, "Difference Methods for Initial Value Problems," p. 101. Wiley (Interscience), New York (1957).
5. C. E. Leith, "Lagrangian Advection in an Atmosphere Model," Lawrence Radiation Laboratory (Livermore) Rept. UCRL-7822, November 1964.